

Article

Research on Subsidence Induced by the Dewatering–Curtain Interaction in the Deep Foundation Pit of the Shield Launching Shaft in Shenzhen, China

Xingsheng Zhang * , Mengke Hu, Xing Chen, Jinyu Dong * and Shipeng Liu

School of Earth Sciences and Engineering, North China University of Water Resources and Electric Power, Zhengzhou 450046, China

* Correspondence: xingsheng.zhang@ncwu.edu.cn (X.Z.); dongjy0552@126.com (J.D.)

Abstract: The waterproof curtain plays an important role in the dewatering of a deep foundation pit. Recognition of the depth of the waterproof curtain inserted into the confined aquifer at different depths may help control ground subsidence due to dewatering, but subsidence analysis of the interaction between dewatering and the waterproof curtain requires further study. In this study, we mainly analyze the relationship between ground subsidence and dewatering based on the shield shaft pit of the Qianhai-Nanshan deep tunnel project in Shenzhen. Our numerical simulation results show that the ground subsidence around the foundation pit decreases with an increase in the depth of the waterproof curtain inserted into the confined aquifer, and when the waterproof curtain completely penetrates the confined aquifer, the ground subsidence caused by pit dewatering is minimal. Our numerical simulation results are consistent with the actual on-site dewatering monitoring data. Our results suggest that the diaphragm wall is an effective measure to control the ground subsidence in deep foundations, helping to reduce excessive dewatering.

Keywords: deep foundation pit dewatering; numerical simulation; diaphragm wall; subsidence



Citation: Zhang, X.; Hu, M.; Chen, X.; Dong, J.; Liu, S. Research on Subsidence Induced by the Dewatering–Curtain Interaction in the Deep Foundation Pit of the Shield Launching Shaft in Shenzhen, China. *Water* **2023**, *15*, 1798. <https://doi.org/10.3390/w15091798>

Academic Editor: Constantinos V. Chrysikopoulos

Received: 11 April 2023

Revised: 29 April 2023

Accepted: 6 May 2023

Published: 8 May 2023



Copyright: © 2023 by the authors. Licensee MDPI, Basel, Switzerland. This article is an open access article distributed under the terms and conditions of the Creative Commons Attribution (CC BY) license (<https://creativecommons.org/licenses/by/4.0/>).

1. Introduction

In recent years, with the acceleration of urbanization in China, the disparity between urban land resources and the increasing demand for construction land has become increasingly prominent. More and more attention has been paid to the development and utilization of underground spaces such as underground transportation hubs, commercial complexes, high-rise basements, and underground drainage tunnels. The corresponding excavation depth and scope of underground space projects have become increasingly greater, and the environmental conditions surrounding foundation pits are becoming more complex [1,2].

Groundwater treatment is the most critical link in deep foundation pit excavation [3]. Improper treatment of groundwater may lead to serious engineering accidents in deep foundation pit projects. Engineering accidents in deep foundation pits will cause huge financial and material resource losses and may even cause the buildings around the foundation pit to sink, crack, or collapse [4–6]. According to reported data on deep foundation pit accidents, the improper treatment of groundwater may cause engineering accidents [7,8]. While dewatering the foundation pit, the ground around the foundation pit experiences a certain degree of subsidence. Therefore, it is necessary to control subsidence around deep foundation pits to reduce the influence of deep foundation pit excavation on surrounding buildings.

In fact, the combined method of well dewatering and the installation of a waterproof curtain is typically used to control the groundwater and ground subsidence. The water-blocking effect of the waterproof curtain is reflected in three aspects: extending the seepage path of groundwater, changing the direction of seepage, and reducing the seepage area [9,10]. The waterproof curtain is divided into a closed waterproof curtain and a

suspended waterproof curtain, depending on whether it completely penetrates the aquifer. A closed waterproof curtain means that the waterproof curtain completely penetrates the aquifer, whereas a suspended waterproof curtain means that the waterproof curtain fails to completely penetrate the aquifer [11]. The suspended waterproof curtain can stop the water mainly by extending the groundwater seepage path such that the groundwater can seep from the bottom of the waterproof curtain towards the foundation pit. The closed waterproof curtain can prevent hydraulic connections between the inside and outside of the pit, playing a significant role in water isolation. The watertightness and ground subsidence control effects of the closed waterproof curtain are better than those of the suspended waterproof curtain. However, when the aquifer is thicker, a suspended waterproof curtain is often used because a closed waterproof curtain is expensive and technically difficult.

Deep foundation dewatering leads to a hydraulic gradient difference between the inside and the outside the foundation pit. The waterproof curtain can prevent more seepage of groundwater from the outside to the inside of the foundation pit through the seepage channel, which can reduce ground subsidence induced by pumping. A few studies have indicated that both the depth of the waterproof curtain and the filter length of the pumping well can reduce ground subsidence outside the waterproof curtain [12]. There are three types of waterproof curtains, including those not inserted into the confined aquifer, those partially inserted into the confined aquifer, and those completely inserted through the confined aquifer. The different relative depths of the waterproof curtain inserted into the confined aquifer produce different effects on groundwater seepage [13].

Some scholars have performed valuable research on the surface subsidence caused by foundation pit dewatering. Yang [14] studied the effective influence depth of incomplete well dewatering and the division of the percolation zone by combining model tests and theoretical analyses, proposing a calculation formula for the outer surface subsidence of the foundation pit. Li [15] analyzed the law of stratum subsidence regarding the foundation pit. Zheng [16] relied on a deep foundation pit dewatering project of the Tianjin Rail Transit Line 5 to reduce the soil subsidence caused by dewatering by setting recharging wells outside the foundation pit for reasonable reinjection. Zhu [17] studied the stratum deformation characteristics of a confined aquifer under the action of depressurization and recharging through a combination of field tests, laboratory tests, and numerical simulation analyses. Zhu [18] conducted an experiment on ground subsidence caused by the pumping of confined water in the Tianjin Binhai New Area, analyzing the laws of subsidence of each stratum during the dewatering process. Three-dimensional numerical and fluid–solid models were used to research the impact of different depths of the diaphragm wall on ground subsidence [19–22].

In this paper, we study the influence of different depths of the waterproof curtain on ground subsidence caused by dewatering, based on the deep foundation pit of the shield launching shaft of the Qianhai-Nanshan deep drainage tunnel in Shenzhen, China. The waterproof curtain used for the pit is the underground diaphragm wall. The actual monitoring data and numerical simulation results are used to compare and analyze the effect of the depth of the diaphragm wall on the dewatering of the foundation pit and ground subsidence around the foundation pit.

2. Background

2.1. Engineering Background

The Qianhai-Nanshan deep drainage tunnel in Shenzhen, China, located in Nanshan district, is located mainly along the west side of Yueliangwan Avenue. The project starts at the current Guankou canal and ends at the water corridor of the Chanwan canal. The initial rainwater and waterlogged water are collected from the Guankou, Zhengbaokeng, and Guimiao canals along the way. The tunnel route intersects more than ten municipal roads from north to south, including Taoyuan Road, Xuefu Road, Guimiao Road, Chuangye Road, Qianwan 1st Road, S3 Guangzhou-Shenzhen Coastal Expressway, and Chanwan

Road. The plan layout of the project location is shown in Figure 1, and the composition of the project construction content is shown in Figure 2.

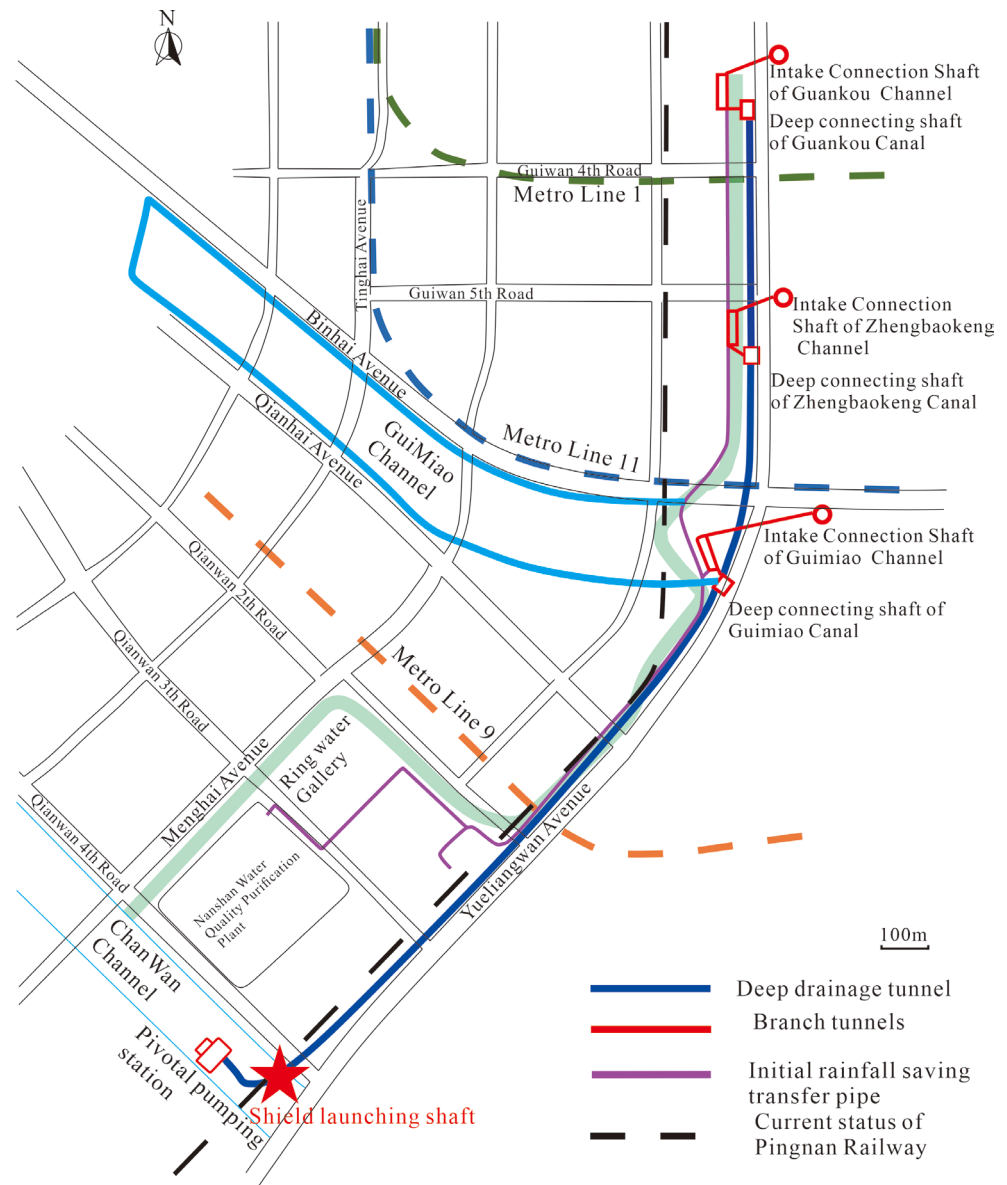


Figure 1. The plan layout of the project location.

The east side of the foundation pit of the shield launching shaft is 70 m away from Yueliangwan Avenue, the west side is marked by the Shenzhen Hong Kong Driving School, the north side is 30 m away from Qianwan Fourth Road, and the south side is an open space. The foundation pit of the shield is a circular open excavation foundation pit, with a diameter of 19.74 m, a ground elevation of 5.6 m, an excavation elevation of -42.45 m, and a foundation pit depth of 48.05 m. The enclosure structure is composed of 267 jet grouting piles to reinforce the pit, 16 groups of diaphragm walls with a thickness of 1.2 m, 1 crown beam, and 5 ring beams. A section of the foundation pit of the shield shaft is shown in Figure 3.

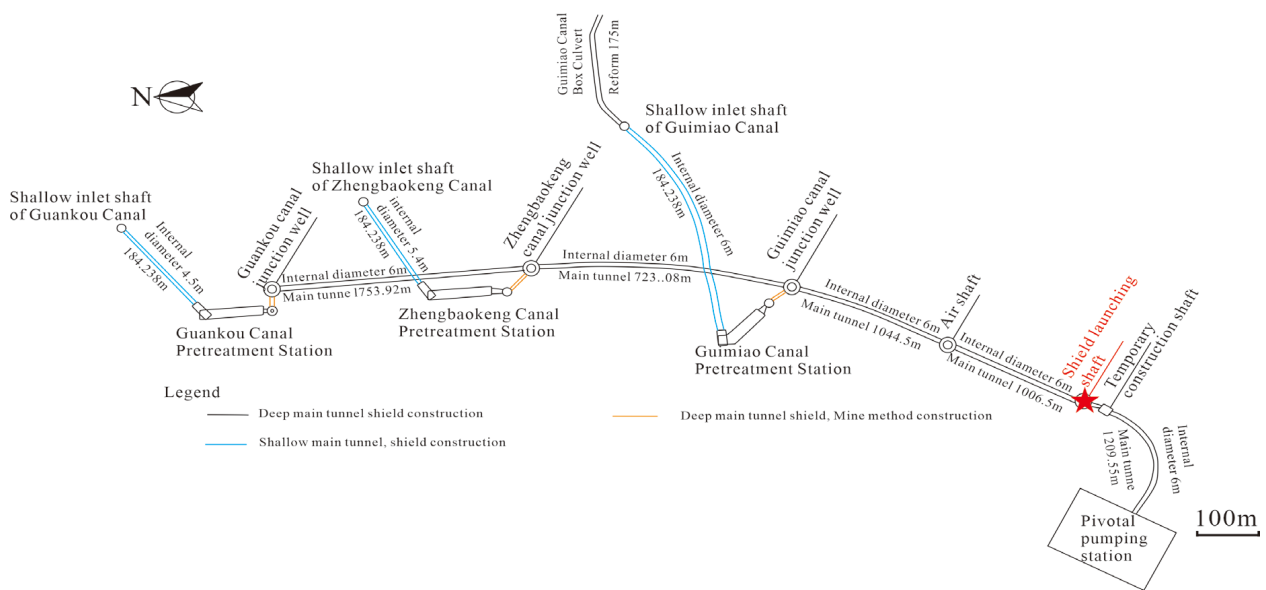


Figure 2. The composition of the project construction content.

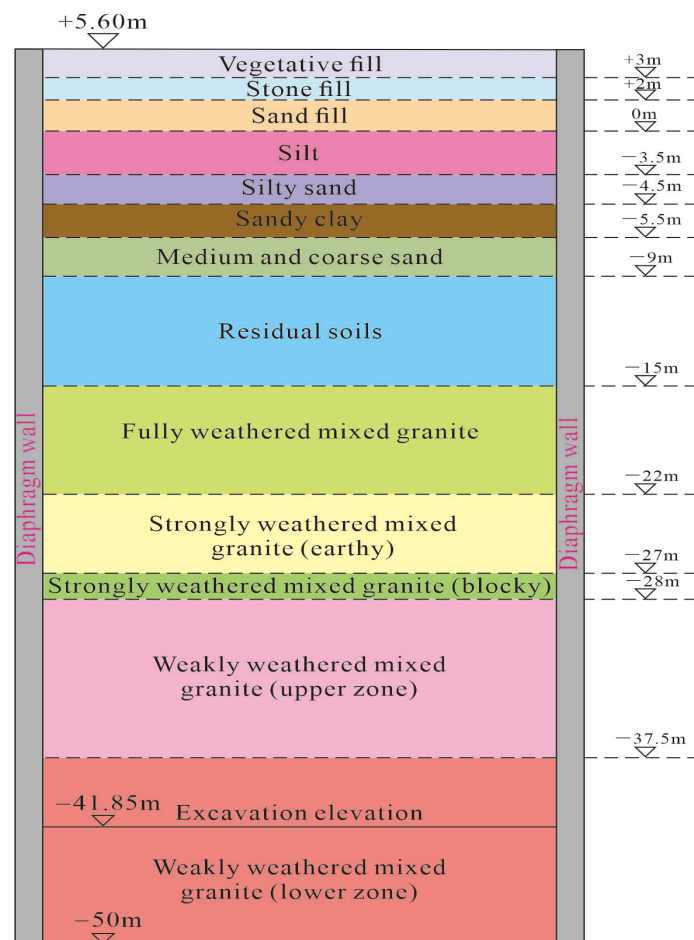


Figure 3. The section of the foundation pit of the shield shaft.

2.2. Strata Distribution

The project is located on the east bank of Qianhai Bay, Shenzhen, China. The origin type of the original landform is the marine accumulation landform and the mixed accumulation landform made up of the sea and the river, from west to east, in order of silty beaches and

marine alluvial plains. Owing to urban expansion and reclamation, most existing sites have become land. Some sections are currently slated for the construction of municipal facilities. The coastal areas are currently subject to construction planning and land reclamation projects. The site is generally flat, and the ground elevation is within 3~11 m. According to regional geological data, the Jixian-Qing Baikou Yinhu group metamorphic rocks, Yanshan Phase IV intrusive rock, and Quaternary Holocene fluvial alluvial and marine terrestrial sedimentary layers are exposed in the area. According to the survey, the parameters of these strata around the foundation pit are shown in Table 1, and their geological profiles are shown in Figure 4.

Table 1. The parameters of each stratum.

Strata Serial	Name of Soil Layer	Elevation of Layer Bottom (m)	Layer Thickness (m)	Average Thickness (m)	Aquifer	Conductivity (cm/s)
①-1	Vegetative fill	−4.50~5.11	0.5~10.5	3.89	Phreatic aquifer	6.84×10^{-3}
①-2	Stone fill	−7.04~4.89	0.4~10.6	3.32		
①-3	Sand fill	−6.29~3.36	0.3~6.8	1.99		
②-1	Silt	−9.64~2.45	0.2~7.0	2.74	Aquitard	6.31×10^{-5}
②-2	Silty sand	−11.11~1.32	0.3~5	1.53	Micro-confined aquifer	3.41×10^{-4}
③-1	Silty clay, sandy clay	−11.00~2.63	0.4~5.7	2.11	Aquitard	9.47×10^{-5}
③-4	Medium-coarse sand	−12.12~−2.79	0.5~6.9	2.79	Micro-confined aquifer	2.40×10^{-2}
④	Residual soils	−34.46~−2.14	0.4~30	6.83		
⑥-1	Fully weathered mixed granite	−40.96~−4.22	0.4~13.55	4.39	Aquitard	5.2×10^{-4}
⑥-2A	Intense weathered mixed granite (soil)	−87.76~−1.86	0.4~46.8	8.12		
⑥-2B	Intense weathered mixed granite (blocky)	−55.16~−2.10	0.4~16.0	3.21	Confined aquifer	1.25×10^{-2}
⑥-3A	Weakly weathered mixed granite (upper zone)	−60.00~−1.15	0.2~22.9	3.96		
⑥-3B	Weakly weathered mixed granite (lower zone)	−63.16~−8.1	0.5~35.1	6.87	Aquitard	2.52×10^{-3}
⑥-4	Slightly weathered mixed granite	−56.15~−8.10	1.6~43.4	14.89		

The excavation depth of the foundation pit is approximately 47.45 m. The upper stratum of the foundation pit shows poor soil stability and cannot be excavated vertically. There are municipal roads and underground pipelines around the site. The foundation pit does not have slope conditions. The underground diaphragm wall, the frame beam, and internal bracing are used for the foundation pit support, and the underground diaphragm wall is also used as the waterproof curtain. The underground diaphragm wall should be inserted to a certain depth under the weakly weathered rock.

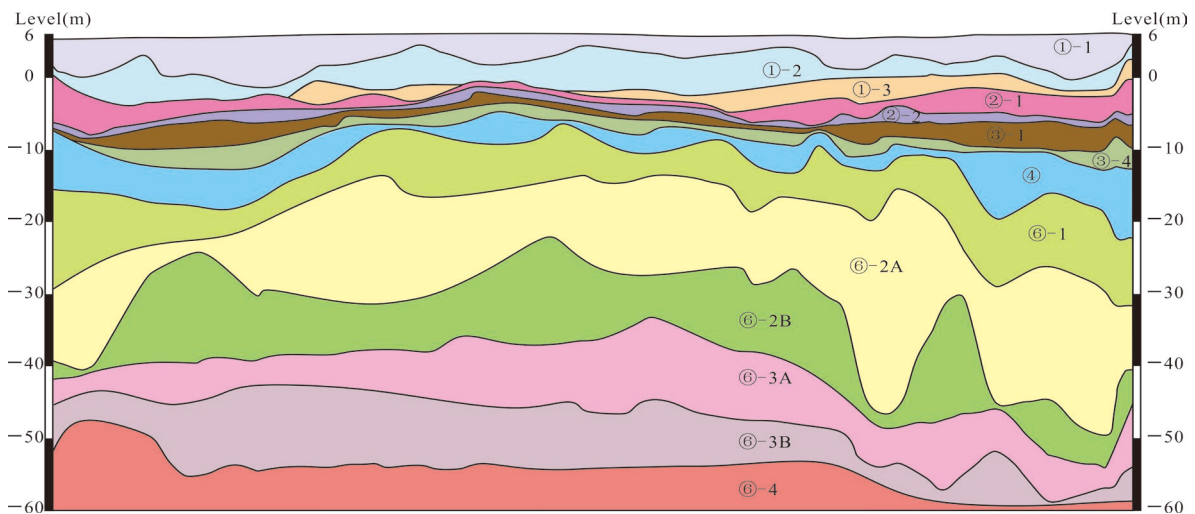


Figure 4. The geological profile.

2.3. Hydrogeological Conditions

The project is located in a southern subtropical maritime climate, which is warm, humid, and rainy. According to rainfall statistics, the average multi-year rainfall is 1593.0 mm, and the annual rainfall is unevenly distributed, mainly concentrated from April to September, accounting for approximately 85% of the annual rainfall, and the distribution of the water system is disordered. Surface water is recharged by seawater during high tide, and there is a hydraulic connection between the surface water and the groundwater in the fill layer. There is good connectivity between the surface water and the groundwater. The groundwater table in the construction area is continuous, and the water surface is more stable. The groundwater table in the dry season is between 2 m and 4 m, and the annual variation of the groundwater table is between 0.5 m and 2 m, which is less influenced by tides and is mainly influenced by rainfall. The groundwater type is Quaternary loose rock pore water and bedrock fissure water. The aquifers in the project area can be divided into the phreatic aquifer, the micro-confined aquifer, and the confined aquifer, according to the burial conditions and the hydraulic state. The buried depth of the groundwater at the site is about 3 m.

Phreatic aquifers mainly include the fill layers (layer ①-1, ①-2, and ①-3). They are mainly recharged by rainfall and groundwater seepage. The average buried depth of the groundwater table is about 3.01 m.

Micro-confined aquifers occur in the alluvial sand layer (layer ②-2 and ③-4). They are mainly recharged by underground lateral seepage and overlaid pore phreatic water leakage. The groundwater is rich and slightly confined. The confined head is low and does not exceed the phreatic water table.

The confined aquifer is mainly located in the weathered fissures of strongly weathered granite to weakly weathered granite, as well as partially opened fracture structure fissures. It exhibits a pressure-bearing property. The groundwater table of the confined aquifer is generally from 4 m to 7 m, the confined water head is from 2.5 m to 37.51 m, and the average confined water head is 24 m below the current surface. The hydraulic conductivities of these layers are listed in Table 1.

The bottom of the diaphragm wall is located in the ⑥-3B weakly weathered mixed granite layer, with a small permeability coefficient belonging a relatively aquitard layer. The excavation depth of the foundation pit is 48.05 m. The bottom of the diaphragm wall of the foundation pit is inserted into the aquitard layer at not less than 8 m. The groundwater table is 2 m below the ground. The groundwater table should be pumped to 2 m below the bottom of the foundation pit. Owing to the action of the diaphragm wall, pumping has little impact on the groundwater fluctuation outside the foundation pit.

3. Numerical Simulations

Mathematical Model

A conceptual model of the Darcy flow, coupled with a diaphragm wall and pumping wells, is provided based on the following assumptions: (1) the confined aquifer is homogeneous and isotropic, with uniform thickness; (2) the vertical flow is negligible; (3) the groundwater seepage follows Darcy's law; (4) both the diaphragm wall and the bottom of the aquifer are impermeable; (5) fluctuations in the strata and seepage from other aquifers are ignored; (6) the original groundwater table is horizontal; and (7) the pore ratio and permeability coefficient remain unchanged during the pumping process [5,23].

A three-dimensional hydro-mechanical coupling model is typically used to predict the amount of ground subsidence, and this model is more accurate in predicting subsidence. The decoupling model, namely the two-step method, can be used for subsidence prediction. In the first step, the drawdown during foundation pit dewatering is calculated using a 3D numerical method. In the second step, surface subsidence is calculated using the consolidation theory [7].

The natural soil mass is a three-dimensional space consisting of solid, liquid, and gas phases; thus, it can be simulated as a porous medium [24]. Therefore, solving the groundwater problem can be simplified by solving the problem of groundwater flow in a porous medium. The continuity equation of groundwater seepage and its definite solution conditions can be used to describe the three-dimensional unsteady seepage law of groundwater [25].

According to the hydrogeological conditions surveyed at this site, the following mathematical model of the three-dimensional unsteady seepage of groundwater can be given:

$$\begin{cases} \frac{\partial}{\partial x} \left(k_{xx} \frac{\partial h}{\partial x} \right) + \frac{\partial}{\partial y} \left(k_{yy} \frac{\partial h}{\partial y} \right) + \frac{\partial}{\partial z} \left(k_{zz} \frac{\partial h}{\partial z} \right) - W = S_s \frac{\partial h}{\partial t} & (x, y, z) \in \Omega \\ h(x, y, z, t)|_{t=0} = h_0(x, y, z) & (x, y, z) \in \Omega \\ h(x, y, z, t)|_{\Gamma_1} = h_0(x, y, z, t) & (x, y, z) \in \Gamma_1 \end{cases} \quad (1)$$

where k_{xx} , k_{yy} , and k_{zz} are the hydraulic conductivities along the x , y , and z directions, respectively. W is the source (L/d), S_s is the specific storage (L/m) of a given point (x , y , z). h is the groundwater table (m) at the given point (x , y , z), t is time (d), Ω is the computational domain, $h_0(x, y, z)$ is the initial groundwater table (m) at point (x , y , z), and Γ_1 is the Dirichlet boundary.

The subsidence caused by dewatering can be given by the following equation:

$$\Delta b = \sum_{i=1}^n b_{0i} m_{vi} s_i \gamma_w F \quad (2)$$

where Δb is the subsidence (mm); b_{0i} is the initial thickness of layer i (m); m_{vi} is the coefficient of the volumetric compressibility of layer i (MPa^{-1}), $m_{vi} = 1/E_i$; s_i is the drawdown of layer i (m); γ_w is the unit weight of groundwater (KN/m^3); F is the empirical subsidence coefficient; and n is the number of layers influenced by dewatering.

4. Numerical Model and Results

4.1. Numerical Model

The three-dimensional finite difference method is preferred for solving mathematical models [26]. We established a numerical model based on the hydrogeological conditions from the geotechnical investigation report and the site pumping test. The simulation area is $2 \text{ km} \times 2 \text{ km}$, with the location of the foundation pit as the center, the ground elevation is 5.6 m, and the depth of the model as 66 m. In order to improve the calculation accuracy, the grids of the numerical model are refined. The numerical model is shown in Figure 5.

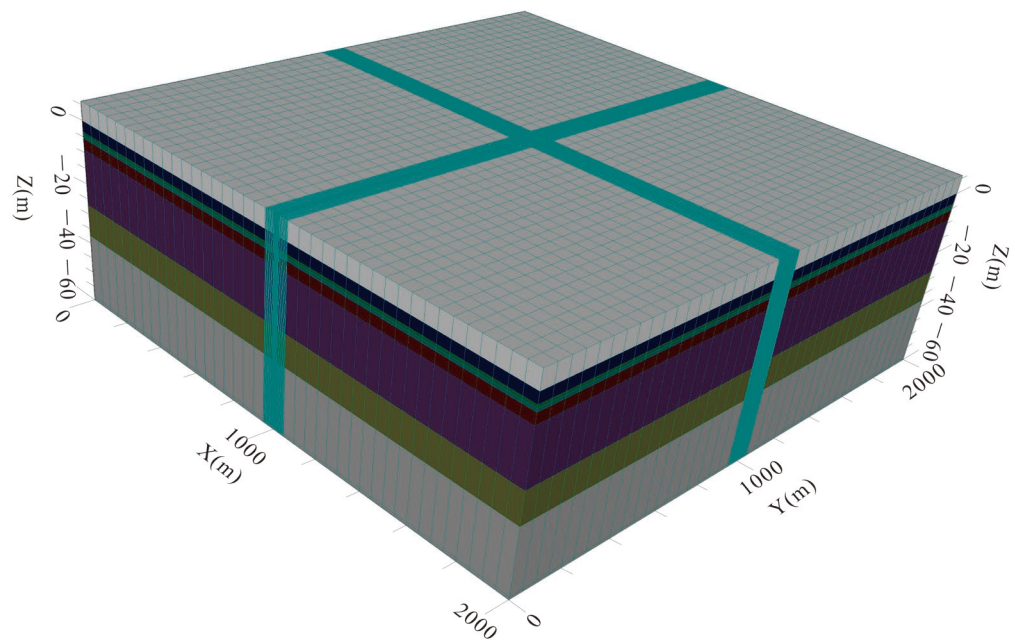


Figure 5. The 3D numerical model.

The soil layer is divided into 8 simulate layers, according to the borehole information, and the permeabilities of the different layers are provided by the field pumping test. The waterproof curtain is simulated by an underground diaphragm wall, with a thickness of 1.2 m and a depth of 56 m below the ground. It is assumed that the diaphragm wall is impermeable in the process of dewatering, and its permeability coefficient is given as 1×10^{-11} m/s. The model is meshed in 50 m units, and the grid size was refined to 2 m near the foundation pit [27]. The final dissected numerical model has 124 rows, 124 columns, and 15,376 active cells.

4.2. Simulation Results

We use visual MODFLOW software to simulate the dewatering project based on the three-dimensional unsteady flow model. Within 500 m outside the foundation pit, the minimum and maximum drawdown of groundwater table are 0.51 m and 0.61 m, respectively. The numerical simulation data and actual data are obtained based on the dewatering design and numerical calculation, as shown in Figure 6. By comparing the head data of the 40 numerical points, it is determined that the calculated head value agrees well with the observed head value. The standard error of the estimated value of the calculated head value and the observed head value is 0.029 m, and the correlation coefficient is 0.998. The drawdown of the confined aquifer outside the foundation pit is shown in Figure 7.

In this paper, we vary the depth of the underground diaphragm wall inserted into the confined aquifer from 10% to 100% of the depth of the confined aquifer. The distribution nephogram of the groundwater table drawdown and the subsidence curves are shown in Figure 7. It can be easily observed from the drawdown nephogram of the groundwater table that as the depth of the diaphragm wall inserted into the confined aquifer increases, the impact of foundation pit dewatering on the groundwater table drawdown outside the foundation pit decreases. The ground subsidence outside the foundation pit decreases as the drawdown of the groundwater table decreases.

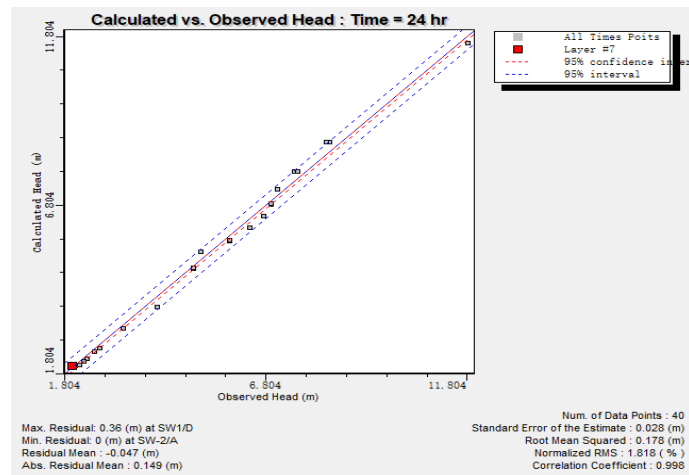
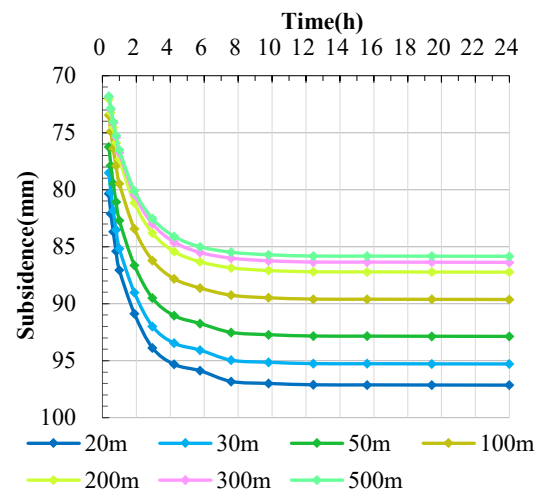
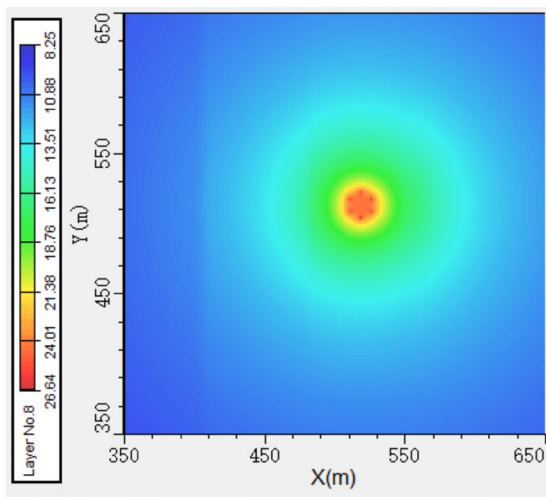


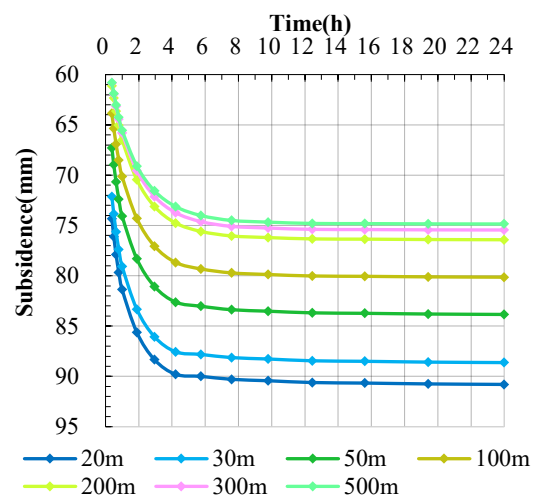
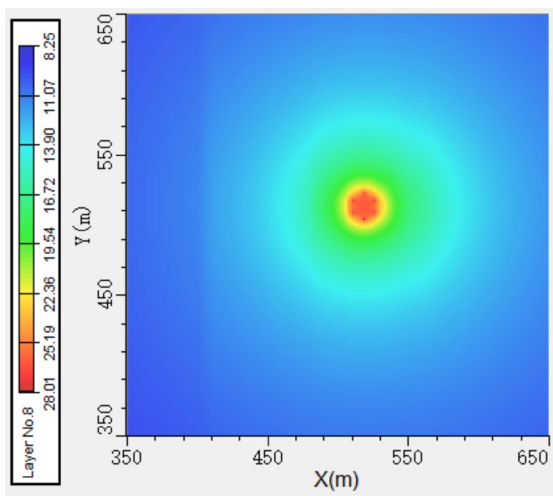
Figure 6. Error analysis diagram.



(1) Spatial distribution of groundwater table drawdown.

(2) Diagram of subsidence curve.

(a) Underground diaphragm wall inserted into 10% of the depth of the confined aquifer.

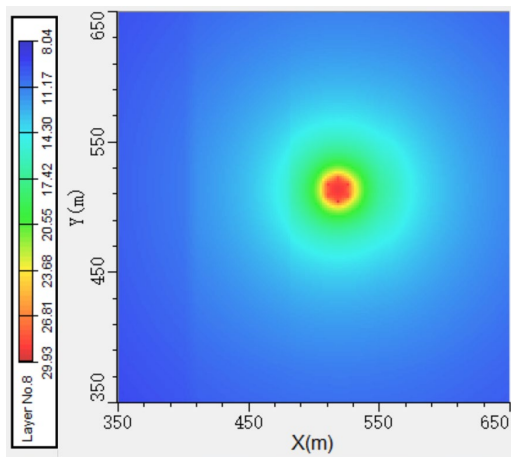


(1) Spatial distribution of groundwater table drawdown.

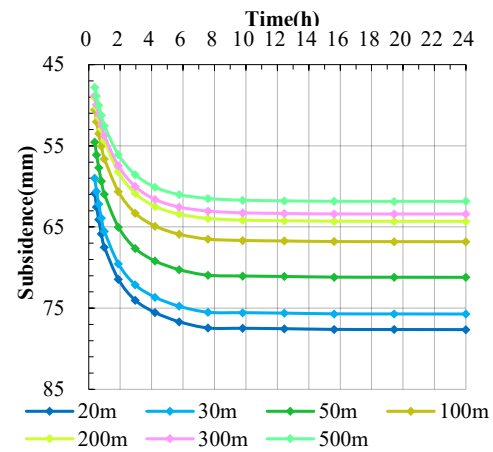
(2) Diagram of subsidence curve.

(b) Underground diaphragm wall inserted into 30% of the depth of the confined aquifer.

Figure 7. Cont.

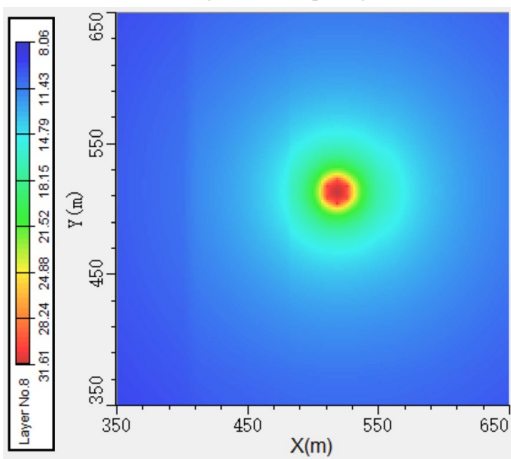


(1) Spatial distribution of groundwater table draw-down.

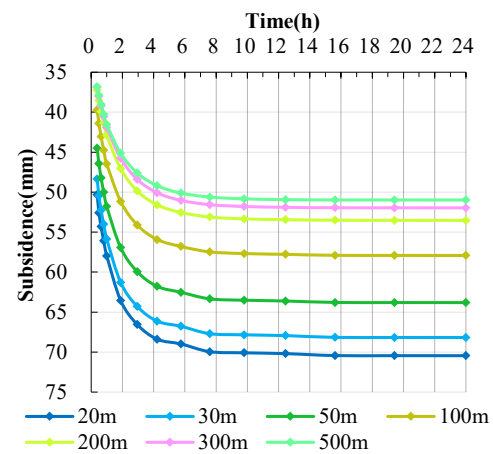


(2) Diagram of subsidence curve.

(c) Underground diaphragm wall inserted into 50% of the depth of the confined aquifer.

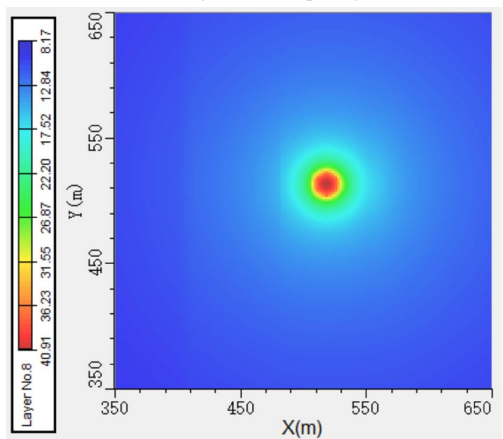


(1) Spatial distribution of groundwater table draw-down.

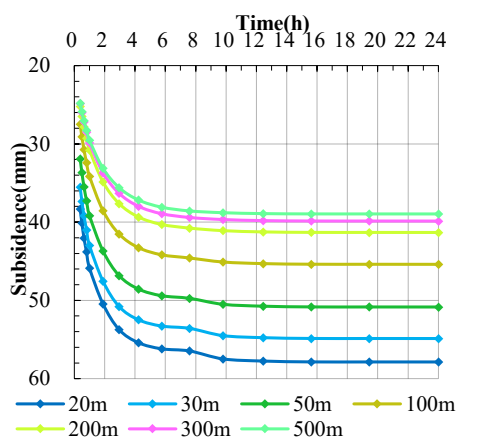


(2) Diagram of subsidence curve.

(d) Underground diaphragm wall inserted into 70% of the depth of the confined aquifer.



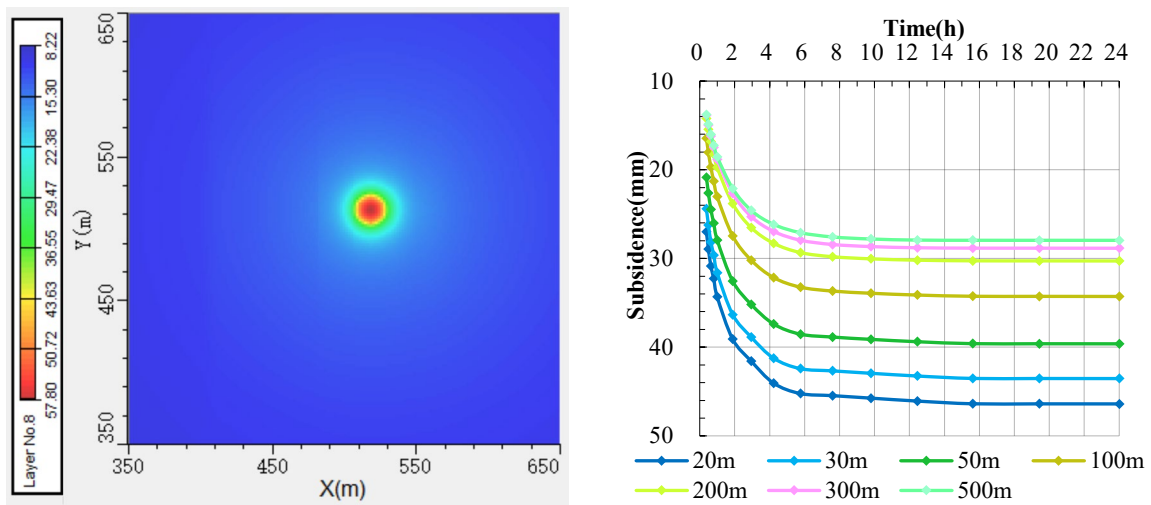
(1) Spatial distribution of groundwater table draw-down.



(2) Diagram of subsidence curve.

(e) Underground diaphragm wall inserted into 80% of the depth of the confined aquifer.

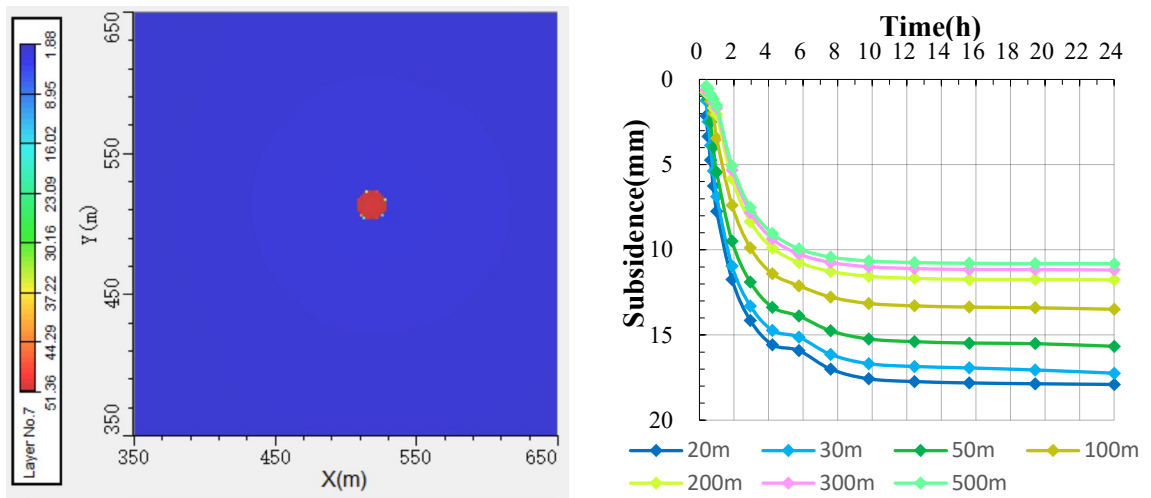
Figure 7. Cont.



(1) Spatial distribution of groundwater table drawdown.

(2) Diagram of subsidence curve.

(f) Underground diaphragm wall inserted into 90% of the depth of the confined aquifer.



(1) Spatial distribution of groundwater table drawdown.

(2) Diagram of subsidence curve.

(g) Underground diaphragm wall inserted into 100% of the depth of the confined aquifer.

Figure 7. Groundwater table and subsidence under the underground diaphragm wall inserted into the confined aquifer at different depths.

Figure 7a is a simulation of 10% of the thickness of the confined aquifer inserted into the underground waterproof wall. Figure 7a(1) shows the nephogram of the drawdown of the groundwater table, and Figure 7a(2) shows the subsidence corresponding to the drawdown of the groundwater table. The analysis results show that the farther away from the foundation pit, the smaller the influence of precipitation on the surface subsidence. Figure 7b shows the underground waterproof wall inserted at 30% of the confined aquifer i. Figure 7b shows that the drawdown of the groundwater table and the ground subsidence have a smaller impact than that in Figure 7a. Figure 7g shows there is a very small impact on the groundwater table and subsidence when the diaphragm wall is fully inserted into the confined aquifer.

Figure 7 shows that the ground subsidence caused by foundation pit dewatering gradually decreases with the increasing of the depth of the underground diaphragm wall inserted into the confined aquifer. According to the results of the nephogram of the groundwater table drawdown in Figure 7a–g, as the depth of the underground diaphragm wall inserted into the confined aquifer gradually increases, the groundwater table drawdown in the foundation pit increases, the influence range of groundwater table drawdown outside the

foundation pit gradually decreases, and the influence on the ground subsidence outside the foundation pit also gradually decreases. When the diaphragm wall is completely inserted into the confined aquifer, the dewatering of the foundation pit has the least influence on the groundwater table drawdown and the ground subsidence outside the foundation pit.

Figure 8 shows that the ground subsidence at one point 200 m away from the foundation pit decreases with an increase in the depth of the underground diaphragm wall inserted into the confined aquifer. Figure 8 shows that ground subsidence changes at a small rate as the depth of the diaphragm wall increases up to 30% of the thickness of the confined aquifer. From Figure 8, it can be seen that the ground subsidence decreased at a greater rate with the increase in the diaphragm wall inserted into the confined aquifer at between 30% and 70% of the thickness of the confined aquifer. Figure 8 shows that ground subsidence decreases at a faster rate with the increase in the diaphragm wall inserted into the confined aquifer at more than 80% of the thickness of the confined aquifer.

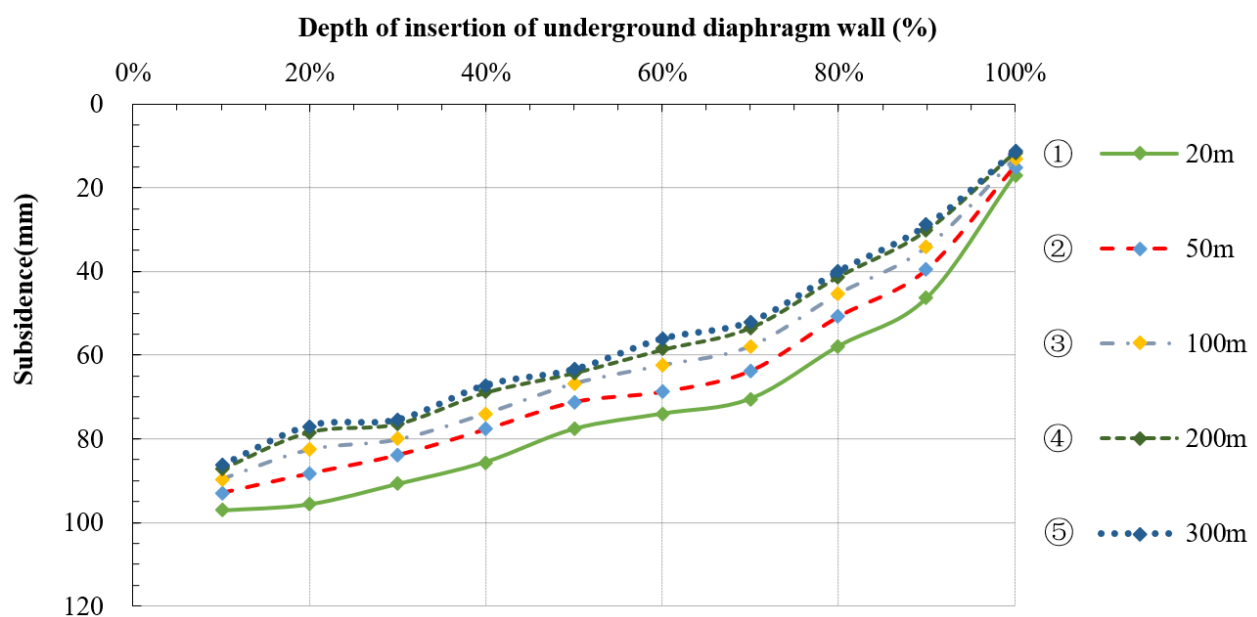


Figure 8. Ground subsidence under the effect of the underground diaphragm wall inserted into confined aquifer at different depths.

5. Conclusions

In this study, we carry out a numerical simulation of the initial stage of the hydro-mechanically coupled processes in a deep foundation pit, including groundwater seepage and ground subsidence. The results of our simulation can be used to quantitatively analyze the law of subsidence caused by the underground diaphragm wall at different depths during the foundation pit dewatering. The effects of different depths of a waterproof curtain on the groundwater table change and surface subsidence in a foundation pit were studied by numerical simulation. The optimal depth of the waterproof curtain inserted into the confined aquifer is obtained through analysis to minimize the ground subsidence value caused by dewatering around the foundation pit. The numerical simulation method, which can consider complex boundary conditions and solve complicated problems in the calculation process, exhibits certain superiorities in the study of foundation pit dewatering, thus providing an effective means for the study of complex foundation pit dewatering problems. Our research regarding the action of a diaphragm wall for controlling groundwater table drawdown and surface subsidence suggests that the diaphragm wall is an effective measure to not only control the ground subsidence in a deep foundation, but also to reduce excessive dewatering, providing an engineering reference for similar local projects.

Author Contributions: X.Z. and M.H. mainly developed the geotechnical numerical model and performed numerical analyses; M.H. gathered in situ data for the geotechnical numerical model; X.Z., M.H., X.C., J.D. and S.L. wrote the main manuscript text; and all authors reviewed and revised the manuscript. All authors have read and agreed to the published version of the manuscript.

Funding: Key R&D and promotion projects in Henan Province (technical research) (No. 202102310018).

Data Availability Statement: All data generated or analyzed during this study are included in the Supplementary Information files and are available from the corresponding author on reasonable request.

Acknowledgments: We thank for the support of Key R&D and promotion projects in Henan Province (technical research) (No. 202102310018).

Conflicts of Interest: The authors declare no conflict of interest.

References

- Jin, L. The use of precipitation technology in the construction of deep foundation pits in buildings. *Pop. Stand.* **2022**, *371*, 149–150, 153.
- Wang, J.X.; Huang, T.R.; Sui, D.C. A Case Study on Stratified Settlement and Rebound Characteristics due to Dewatering in Shanghai Subway Station. *Sci. World J.* **2013**, *2013*, 213070. [[CrossRef](#)]
- Xu, Y.S.; Shen, S.L.; Ren, D.J.; Wu, H.N. Analysis of Factors in Land Subsidence in Shanghai: A View Based on a Strategic Environmental Assessment. *Sustainability* **2016**, *8*, 573. [[CrossRef](#)]
- Li, W.; Zhang, Y.Y.; Zhang, Y.Y.; Li, X.; Shen, C. Research on the Deep Foundation Pit Dewatering Design by Three-dimensional Numerical Simulation. *Urban Geotech. Investig. Surv.* **2019**, *1*, 189–192. (In Chinese)
- Wang, J.; Huang, T.; Hu, J.; Wu, L.; Li, G.; Yang, P. Field experiments and numerical simulations of whirlpool foundation pit dewatering. *Environ. Earth Sci.* **2014**, *71*, 3245–3257. [[CrossRef](#)]
- Wang, J.; Wu, Y.; Liu, X.; Yang, T.; Wang, H.; Zhu, Y. Areal subsidence under pumping well–curtain interaction in subway foundation pit dewatering: Conceptual model and numerical simulations. *Environ. Earth Sci.* **2016**, *75*, 198. [[CrossRef](#)]
- Katzenbach, R.; Leppla, S.; Ramm, H.; Seip, M.; Kuttig, H. Rolf KatzenbachSteffen LepplaHeiko Kuttig. Design and Construction of Deep Foundation Systems and Retaining Structures in Urban Areas in Difficult Soil and Groundwater Conditions. *Procedia Eng.* **2013**, *57*, 540–548. [[CrossRef](#)]
- Wang, J.; Feng, B.; Liu, Y.; Wu, L.; Zhu, Y.; Zhang, X.; Tang, Y. Controlling subsidence caused by de-watering in a deep foundation pit. *Bull. Eng. Geol. Environ.* **2012**, *71*, 545–555. [[CrossRef](#)]
- Zhang, Z.H.; Guo, Y.C.; Fan, Q.H.; Zhang, Q.X. Calculation Method for Land Subsidence Induced by Dewatering of Foundation Pit with Suspended Waterproof Curtains. *J. Northeast. Univ. Nat. Sci.* **2021**, *42*, 1329–1334. (In Chinese)
- Mana, D.S.K.; Gourvenec, S.; Randolp, M.F. Numerical modelling of seepage beneath skirted foundations subjected to vertical uplift. *Comput. Geotech.* **2014**, *55*, 150–157. [[CrossRef](#)]
- Zhang, Q.X.; Wei, M.; Wang, C.M. Numerical Simulation of Groundwater Seepage in Suspended. *Geotech. Eng.* **2021**, *35*, 146–150, 156. (In Chinese)
- Wang, X.W.; Yang, L.T.; Xu, S.Y.; Shen, S.L. Evaluation of optimized depth of waterproof curtain to mitigate negative impacts during dewatering. *J. Hydrol.* **2019**, *577*, 123969. [[CrossRef](#)]
- Li, W.; Tong, L.Y.; Wang, Z.S.; Liu, S.Y.; Zhang, M.F. Analysis of Impact of Dewatering on the Environment under Different Inserted Depth of Diaphragm Wall. *Chin. J. Undergr. Space Eng.* **2015**, *11* (Suppl. 1), 272–277. (In Chinese)
- Yang, Q.Y.; Zhao, B.M. Experimental and theoretical study on the surface subsidence by dewatering of foundation pit in phreatic aquifer. *Chin. J. Rock Mech. Eng.* **2018**, *37*, 15061519. (In Chinese) [[CrossRef](#)]
- Li, Y.; He, Z.Z.; Yan, G.H.; Liao, Z.Y.; Liang, S.Y. Excavation dewatering and ground subsidence in dual structural stratum of Wuhan. *Chin. J. Geotech. Eng.* **2010**, *34* (Suppl. 1), 767–772. (In Chinese)
- Zheng, G.; Zhao, Y.B.; Cheng, X.S.; Ha, D.; Li, Q.H. Strategy and analysis of the settlement and deformation caused by dewatering under complicated geological condition. *Chin. J. Geotech. Eng.* **2019**, *52* (Suppl. 1), 135–142. [[CrossRef](#)]
- Zhu, Y.F. Mechanism and control analysis of strata deformation induced by confined water pumping and recharging. *Shanghai Jiao Tong Univ.* **2016**. (In Chinese)
- Can, Z.H.U.; Zhang, Y.; Guofeng, H.E. In-situ tests of land subsidence caused by pumping in the Tianjin Binhai New Area. *Hydrogeol. Eng. Geol.* **2018**, *45*, 159–164.
- Chen, Z.H.; Huang, J.T.; Zhan, H.B.; Wang, J.G.; Dou, Z.; Zhang, C.J.; Chen, C.S.; Fu, Y.S. Optimization schemes for deep foundation pit dewatering under complicated hydrogeological conditions using MODFLOW-USG. *Eng. Geol.* **2022**, *303*, 106653. [[CrossRef](#)]
- Wang, J.X.; Liu, X.T.; Wu, Y.B.; Liu, S.L. Field experiment and numerical simulation of coupling non-Darcy flow caused by curtain and pumping well in foundation pit dewatering. *J. Hydrol.* **2017**, *549*, 277–293. [[CrossRef](#)]
- Zeng, C.F.; Wang, S.; Xue, X.L.; Zheng, G.; Mei, G.X. Evolution of deep ground settlement subject to groundwater drawdown during dewatering in a multi-layered aquifer-aquitard system: Insights from numerical modelling. *J. Hydrol.* **2021**, *603*, 127078. [[CrossRef](#)]

22. Xu, Y.S.; Ma, L.; Shen, S.L.; Sun, W.J. Evaluation of land subsidence by considering underground structures that penetrate the aquifers of Shanghai, China. *Hydrogeol. J.* **2012**, *20*, 1623–1634. [[CrossRef](#)]
23. Yang, K.F.; Xu, C.J.; Chi, M.L. Analytical Analysis of the Groundwater Drawdown Difference Induced by Foundation Pit Dewatering with a Suspended Waterproof Curtain. *Appl. Sci.* **2022**, *12*, 10301. [[CrossRef](#)]
24. Zhao, S.Z.; Song, G. Application of ModFlow to precipitation simulation in extra deep foundation pit. *Shanxi Archit.* **2011**, *37*, 51–52. (In Chinese)
25. Liu, Z.W. Three-dimensional Numerical Simulation Analysis of Deep Foundation Pit Dewatering of Metro Station. *Urban Geotech. Investig. Surv.* **2020**, *6*, 187–192. (In Chinese)
26. Wang, J.; Feng, B.; Guo, T.; Wu, L.; Lou, R.; Zhou, Z. Using partial penetrating wells and curtains to lower the water level of confined aquifer of gravel. *Eng. Geol.* **2013**, *161*, 16–25. [[CrossRef](#)]
27. Lv, S.G. Design and impact analysis of foundation pit precipitation based on Visual Modflow software. *Sichuan Cem.* **2021**, *3*, 278–279.

Disclaimer/Publisher’s Note: The statements, opinions and data contained in all publications are solely those of the individual author(s) and contributor(s) and not of MDPI and/or the editor(s). MDPI and/or the editor(s) disclaim responsibility for any injury to people or property resulting from any ideas, methods, instructions or products referred to in the content.